



ANNUAL
REVIEWS **Further**

Click [here](#) to view this article's online features:

- Download figures as PPT slides
- Navigate linked references
- Download citations
- Explore related articles
- Search keywords

Shear Banding of Complex Fluids

Thibaut Divoux,¹ Marc A. Fardin,²
Sebastien Manneville,³ and Sandra Lerouge⁴

¹Centre de Recherche Paul Pascal, CNRS UPR 8641, Université de Bordeaux, 33600 Pessac, France

²Institut Jacques Monod, CNRS UMR 7592, Université Paris-Diderot, 75205 Paris Cédex 13, France

³Laboratoire de Physique, École Normale Supérieure de Lyon, Université de Lyon, CNRS UMR 5672, 69364 Lyon Cédex 07, France

⁴Laboratoire Matière et Systèmes Complexes, CNRS UMR 7057, Université Paris-Diderot, 75205 Paris Cédex 13, France; email: sandra.lerouge@univ-paris-diderot.fr

Annu. Rev. Fluid Mech. 2016. 48:81–103

First published online as a Review in Advance on July 22, 2015

The *Annual Review of Fluid Mechanics* is online at fluid.annualreviews.org

This article's doi:
10.1146/annurev-fluid-122414-034416

Copyright © 2016 by Annual Reviews.
All rights reserved

Keywords

heterogeneous flows, flow instabilities, shear-induced transitions, polymeric fluids, yield stress fluids, delayed yielding

Abstract

Even in simple geometries, many complex fluids display nontrivial flow fields, with regions where shear is concentrated. The possibility for such shear banding has been known for several decades, but in recent years, we have seen an upsurge in studies offering an ever-more precise understanding of the phenomenon. The development of new techniques to probe the flow on multiple scales with increasing spatial and temporal resolution has opened the possibility for a synthesis of the many phenomena that could only have been thought of separately before. In this review, we bring together recent research on shear banding in polymeric and soft glassy materials and highlight their similarities and disparities.

1. INTRODUCTION

Shear banding seems to have been first identified at the end of the nineteenth century by geologists and engineers working on the deformation of solids (Wright 2002). In this context, shear bands are zones in which the strain γ can take values much larger than in the rest of the sample. The present review focuses on shear banding in complex fluids, which are part of what one may call soft matter (de Gennes 1992): a somewhat overlapping collection of systems such as liquid crystals, colloidal dispersions, polymer solutions, melts or gels, emulsions, pastes, and foams (Larson 1999). In all these systems, the constituents are often said to be mesoscopic because the relevant length scale, which in practice is not always clearly identified, ranges between the molecular scale and the flow scale. Macroscopically, the mechanical properties of soft matter sit in between those of the ideal Hookean elastic solid and those of the ideal Newtonian viscous fluid. In this context, the notion of shear banding is associated with the localization of the shear (or strain) rate $\dot{\gamma}$.

Shear banding is ubiquitous in complex fluids and has been reported in systems such as wormlike micellar surfactant solutions, lyotropic lamellar surfactant phases, polymer solutions and melts, star polymers, emulsions, suspensions, microgels, biological gels, and foams. Several reviews have been published in recent years concerning various theoretical and experimental aspects. For instance, in the *Annual Review of Fluid Mechanics*, the topic was last approached by Goddard (2003), from a mechanistic perspective grounded in the historical background on shear banding in solids, and more recently by Schall & van Hecke (2010), who mainly focused on recent experiments on shear banding in granular matter. Over the five years since the latter publication, more than 500 articles mentioning the terms shear banding and complex fluids have been published. This profusion of studies reflects the growing interest for this subject and justifies the need for a new review today. This profusion is also a consequence of the very broad, but sometimes loose, use of the term shear banding. The words chosen in particular research fields may be somewhat contextual, and determining whether two words across fields are synonyms is not always easy. Some of what other authors have called layers, stripes, fractures, or even kinks may be close to our use of the term bands in this review, and vice versa. Our goal is not to authoritatively define what shear banding is and is not, but to witness the evolution, and refinement over the use, of the term shear banding in recent soft matter research.

In practice, we do not cover the 500 references of the past five years, but we focus on two classes of materials: polymeric fluids (Section 2) and soft glassy materials (Section 3). The first class of materials sits more on the side of fluids, whereas the second sits more on the side of solids. Our examples are typically dominated by shear rather than elongation. Nonetheless, phenomena such as extensional necking (Fielding 2011) are analogous to what could be called elongation banding, and many of the phenomena mentioned in a review about shear-dominated flows could be carried over to elongation-dominated flows.

2. SHEAR BANDING IN POLYMERIC FLUIDS

In this section, we discuss shear banding in polymeric fluids, chiefly polymer and surfactant wormlike micellar solutions. We focus on the semidilute and concentrated regimes in which polymeric chains form a viscoelastic entangled network. At or close to equilibrium, polymer and micellar solutions present a formal analogy: They follow simple scaling laws as a function of concentration, and they exhibit similar phase behaviors. The main differences lie in the ability of wormlike micelles to break and recombine, a quality that earned them the name of living polymers. The analogy can be taken further when considering the rheology of these systems, especially because

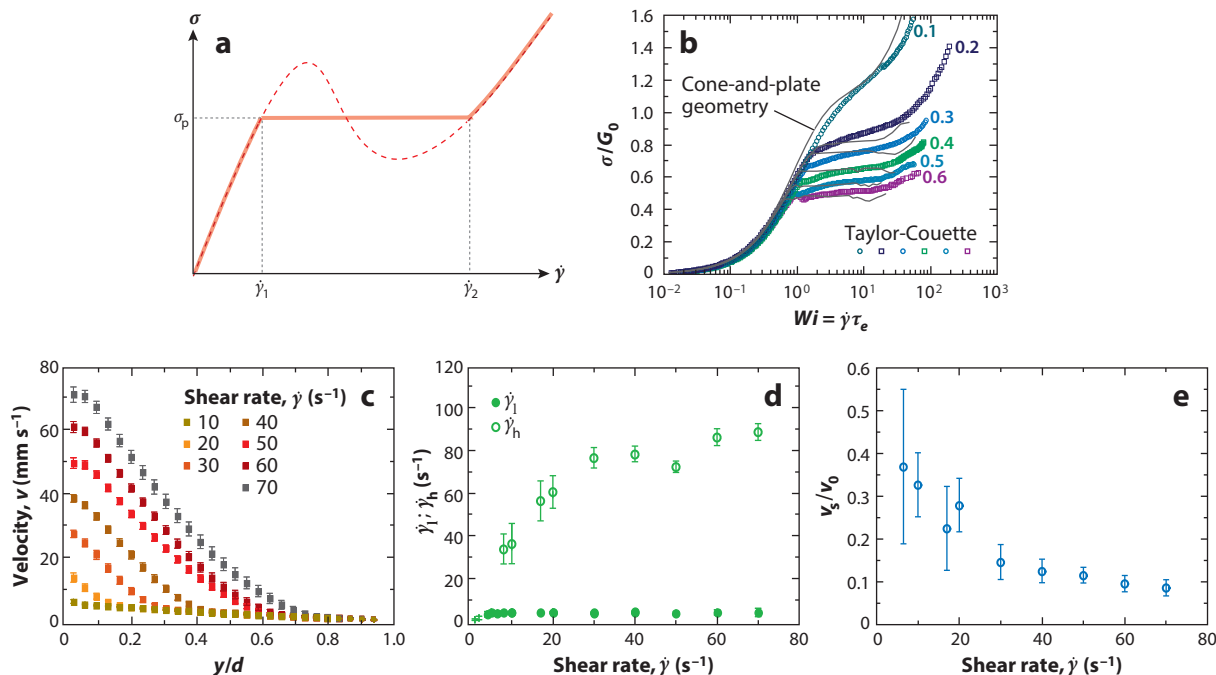


Figure 1

(a) Schematic flow curve of a complex fluid undergoing a shear-banding transition according to the material instability scenario. The measured flow curve is made of two branches, a priori stable, separated by a stress plateau ($\sigma = \sigma_p$). The underlying constitutive curve is nonmonotonic. (b) Typical set of experimental steady-state flow curves of wormlike micellar solutions obtained for various molar surfactant concentrations by increasing the imposed shear rate. The shear stress σ is in units of the elastic modulus G_0 , and the dimensionless shear rate is the Weissenberg number $Wi \equiv \dot{\gamma}\tau_e$, where τ_e is the relaxation time of the fluid. Symbols and lines correspond to flow curves obtained in a Taylor-Couette device and in cone-and-plate geometry, respectively. Panel b adapted with permission from Fardin et al. (2012c), copyright by the Royal Society of Chemistry. (c) Typical time-averaged velocity profiles gathered in Taylor-Couette flow using ultrasonic velocimetry for different applied shear rates along the stress plateau. (d) Mean local shear rates $\dot{\gamma}_l$ and $\dot{\gamma}_h$ estimated from a linear fit of the velocity profile $v(y)$ in each band as a function of the applied shear rate. (e) Mean slip velocity v_s measured at the inner moving cylinder as a function of $\dot{\gamma}$. Panels c–e adapted with permission from Fardin & Lerouge (2012), copyright by Springer-Verlag.

the original models that are able to capture much of their rheological features all originated from the tube model (Doi & Edwards 1988).

Historically, shear banding was first predicted and observed in this class of complex fluids, which still constitutes a strong guide for the emergence of this phenomenon in other types of systems. In the context of solid mechanics, shear bands have been understood as a consequence of a material instability (Goddard 2003), which results—at the macroscopic continuum scale—from nonmonotonic constitutive relations. For fluids, constitutive laws are first and foremost probed by measuring the flow curve (i.e., the relationship between shear stress and shear rate in viscometric flows). If a fluid displays a nonmonotonic flow curve, such as the one sketched in **Figure 1a**, the range of shear rate with decreasing shear stress is mechanically unstable (Yerushalmi et al. 1970). Such a curve is evidently not found in experiments but is computed theoretically by enforcing the homogeneity of the shear rate. In practice, the stress plateaus to a value σ_p above a critical shear rate $\dot{\gamma}_l$, and the flow splits into domains bearing high ($\dot{\gamma}_h$) and low ($\dot{\gamma}_l$) shear rates, with the low and

high local shear rates connected to the low ($\dot{\gamma}_1$) and high ($\dot{\gamma}_2$) bounds of the global stress plateau. In simple shear flows, the viscosities in the high- and low-shear rate bands are $\eta_h \sim \sigma_p/\dot{\gamma}_h$ and $\eta_l \sim \sigma_p/\dot{\gamma}_l$. That the local viscosities are changing is a testimony to the fact that the structure of the fluid is changing. In this context, the shear-banding instability is often associated with shear-induced structuration of the fluid.

The possibility for such material instability in fluids first emerged in research by Vinogradov (1973) on the spurt effect in polymer solutions and melts (i.e., the dramatic increase of the flow rate above a critical pressure drop during extrusion out of a conduit). The idea that the spurt effect could be a consequence of the existence of shear banding was later formalized, in particular, by McLeish & Ball (1986), who highlighted that the then-recently developed Doi-Edwards (tube) theory of polymer dynamics did predict a nonmonotonic flow curve (Doi & Edwards 1988). The problem with this hypothesis was that the many experiments on polymers in viscometric conditions had not reported any nonmonotonic or discontinuous flow curve, and a fortiori no shear banding (Bird et al. 1987). From this discrepancy between theory and experiments, two routes were taken in parallel. On the one side, additions were made to the tube theory to take into account the kinetics of breaking/recombination in wormlike micelles (Cates 1990), in which broad stress plateaus hinting at the presence of shear banding were beginning to be observed in experiments (Rehage & Hoffmann 1991). This was the starting point of intensive experimental research sustained by strong theoretical feedback. On the other side, the tube model was refined to better reflect the dynamics of polymers and to cure the original model of its nonmonotonicity (Marrucci 1996). In parallel, experiments were conducted to support (or not) the theoretical picture, which was also updated regularly.

In what follows, we summarize the major advances in the field over the past 10 years. We first discuss the successes and difficulties in correlating extensive sets of data for shear-banding wormlike micelles, providing a road map for future investigations on other complex fluids. We then turn to polymer solutions and melts, for which the existence of shear banding is still a controversial subject. Finally, we give an overview on the theoretical modeling of shear banding in polymeric fluids at large.

2.1. Correlating Data Sets of Increasing Subtlety in Wormlike Micelles: A Road Map for Other Complex Fluids

The nonmonotonic flow curve sketched in **Figure 1a** is a powerful picture to understand shear banding; it is quite general and applies to many types of flows and fluids. On this basis, purely rheometric experiments showed that for a given solution of wormlike micelles at a given temperature, the stress plateau was unique but could be influenced by the flow geometry. This became an important theoretical problem, which we discuss further in Section 2.3. However, this sketch is essentially zero dimensional (0D) in the sense that it is obtained by imposing the tensorial strain rate field to be a pure shear rate field, constant and equal to the global shear rate signal $\bar{\dot{\gamma}}$. Space has disappeared from the picture, and because the flow curve is assumed to be steady, time is not mentioned either.

It quickly became obvious that one had to go beyond this 0D picture, and a collective effort was made to combine purely rheometric data with more mesoscopic, local, and nonmechanical data (chiefly optical and structural data). Direct evidence for shear-banded flows associated with the coexistence of differing microstructures was then supported by flow birefringence (FB), small-angle neutron scattering (SANS), and nuclear magnetic resonance (NMR) velocimetry and spectroscopy experiments. For exhaustive references about that part of the story, the reader can refer to Berret (2006) and Lerouge & Berret (2010). Heterogeneous flows have been probed in

various flow geometries, such as pipe (Mair & Callaghan 1997), cone and plate (CP) (Britton & Callaghan 1997), Taylor–Couette (TC) (Salmon et al. 2003a), and more recently microchannel (Nghe et al. 2010, Ober et al. 2011).

Our understanding of shear-banded flows in wormlike micelles is particularly advanced in TC flow, in the small-gap limit, because this canonical geometry turned out to be the most suitable for the implementation of powerful space- and time-resolved techniques (Callaghan 2008, Manneville 2008, Eberle & Porcar 2012). Moreover, it presents additional advantages: The slight stress inhomogeneity due to curvature tends to produce a plateau with a slight positive incline (**Figure 1b**), such that both the stress and shear rate can be used as control parameters. It also pushes the shear-banding flow to comprise only two bands, with the high–shear rate band always near the inner cylinder (radius R). In contrast, in a CP flow, there can be two, three, or even more bands, and their location is more variable (Britton & Callaghan 1997, Boukany & Wang 2008, Casanellas et al. 2015). TC flow is less prone to edge effects, which can strongly limit the accessible range of flow strength in CP flow, for instance (Dimitriou et al. 2012). **Figure 1c** displays typical time-averaged velocity profiles gathered in TC flow as a function of the radial distance y to the inner cylinder normalized by the gap width d . Such velocity profiles now provide what we could call a 1D picture.

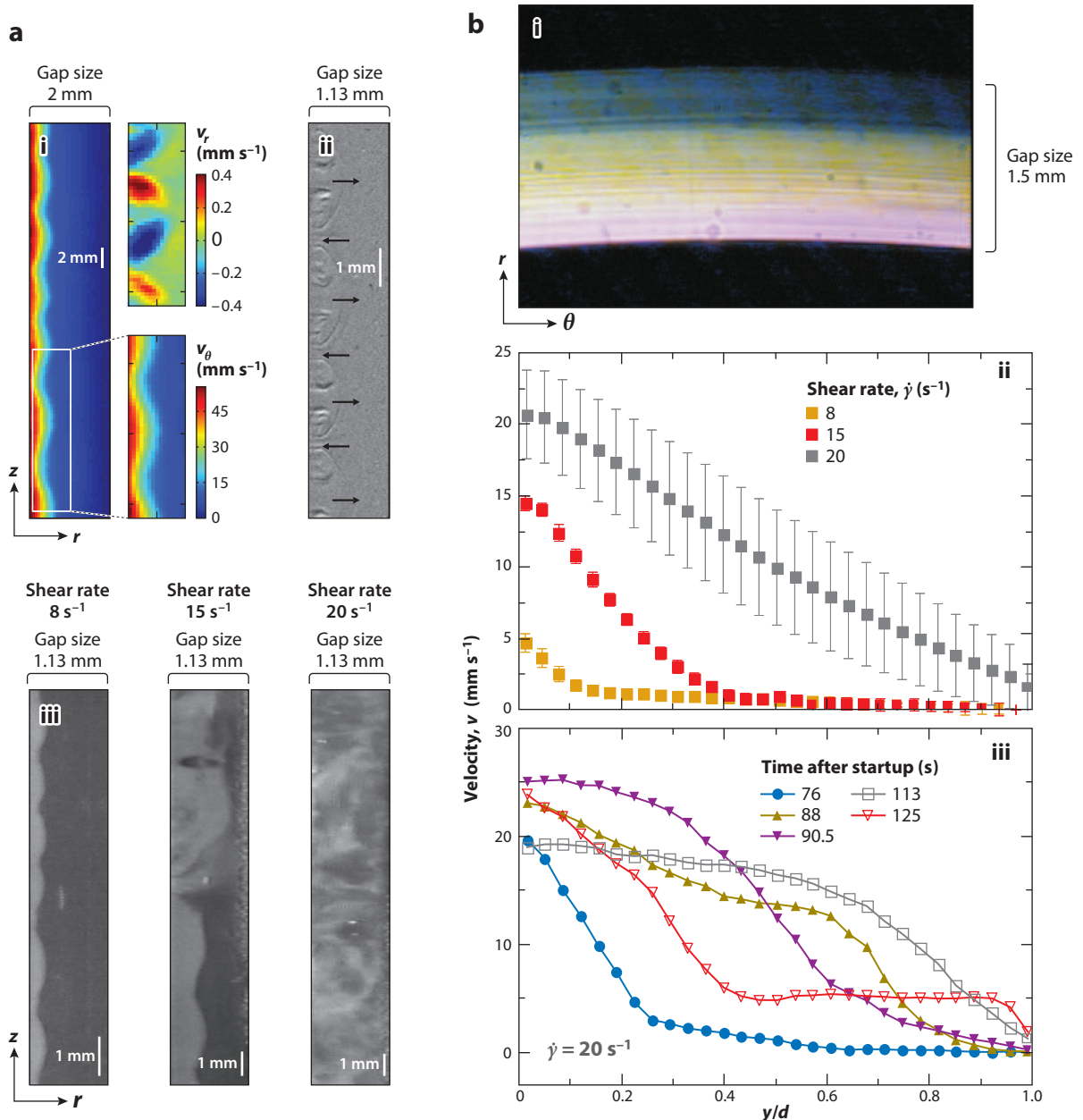
The early 1D experiments (Salmon et al. 2003a) were mostly focused on the simple assumptions made in theoretical modeling: no wall slip, an infinitely sharp interface, and the lever rule (Spenley et al. 1996), which constitute the so-called classical scenario. With the refinement of spatial and temporal accuracy, we now understand these assumptions to be simplistic. Wall slip on the high–shear rate band seems quite deeply connected to shear banding and leads to deviations from the original lever rule (Radulescu et al. 1999, Fardin et al. 2012b). In particular, the local high shear rate is usually observed to be somewhat in competition with wall slip (Lettinga & Manneville 2009, Feindel & Callaghan 2010, Fardin et al. 2012a). It increases with the applied shear rate, as the dimensionless wall slip is concomitantly reduced (**Figure 1d,e**). This feature emerges even in the simplest theories of shear banding because of the coupling between the diffusive terms and the boundary conditions (Cromer et al. 2011, Fardin et al. 2012b). As for the width of the interface ℓ , it is thin in comparison to the usual gap ($d \simeq 1$ mm), but it is larger than what was once thought (Radulescu et al. 2003) and is typically measured to be 1–10 μm (Ballesta et al. 2007). In microfluidic devices, the existence of such a length scale leads to so-called nonlocal effects (Masselon et al. 2010).

This 1D picture has also been developed on the structural side. Orientation profiles were established using FB (Lerouge et al. 2004), NMR spectroscopy (López-González et al. 2006), and more recently SANS (Helgeson et al. 2009, Gurnon et al. 2014). They all showed consistency, with flow-aligned wormlike micelles in the high–shear rate band coexisting with entangled wormlike micelles in the low–shear rate band for semidilute samples and with a shear-induced isotropic-to-nematic transition for concentrated samples, with possibly concentration differences between bands for the latter case.

With the improvement of time resolution, local velocity fluctuations and complex motions of the bands have been reported in many different wormlike micellar systems, often coupled to non-stationary responses of the global rheological signals (Lerouge et al. 2000, López-González et al. 2004, Hu & Lips 2005, Ganapathy & Sood 2006, Bécu et al. 2007, Fielding 2007). Understanding of these complex fluctuating dynamics recently came from the extension of the experiments to two dimensions, two dimensions plus time, and so on. Indeed, in the 1D picture, the velocity component in the flow direction is obtained at one given height along the cylinders, whereas FB and SANS data are gathered by averaging along the vorticity direction. These specifications are now seen as quite limiting, and sometimes even misleading. The fluctuations in shear-banding

Lever rule: in the classical scenario, written as $\dot{\gamma} = (1 - \alpha_h)\dot{\gamma}_l + \alpha_h\dot{\gamma}_h$, with α_h the proportion of the high–shear rate band, $\dot{\gamma}_l = \dot{\gamma}_1$ and $\dot{\gamma}_h = \dot{\gamma}_2$

wormlike micelles were shown to mainly result from the development, in the high-shear rate band, of secondary flows that are either coherent and associated with interfacial undulations along the vorticity direction (Lerouge et al. 2008) or turbulent (Fardin et al. 2009, 2012a; Perge et al. 2014) (**Figure 2a**). The impact of such 3D shear-banding flows on the 1D picture was fully characterized (**Figure 2b**), demonstrating the ubiquity of this phenomenon (Fardin & Lerouge 2012), which was shown to originate from viscoelastic instabilities driven by normal stresses akin to those well known to develop in polymer solutions in flows with curved streamlines (Morozov & van



Saarloos 2007, Muller 2008). The most recent experiments and simulations have suggested that in curved shear-banded flows, bulk and interfacial viscoelastic instabilities can be at play, with the bulk mechanism dominant except when the effective curvature of the high-shear rate band is vanishing (Decruppe et al. 2010, Fielding 2010, Fardin et al. 2011, Nicolas & Morozov 2012). These recent advances may provide a strong guide for the understanding of complex shear banding in other flow geometries.

2.2. Shear Banding in Polymer Solutions and Melts

As mentioned in Section 2, despite the success of the tube theory in capturing much of the rheology of entangled polymer solutions and melts, for a long time shear banding was not reported in these systems (Menezes & Graessley 1982, Bercea et al. 1993, Pattamaprom & Larson 2001). All the early studies were purely rheometric, echoing the purely mechanical instability illustrated by the 0D picture. As shear banding was not observed, theoreticians worked on updating the original tube model (see McLeish 2002 for a review). One of the additions that is particularly relevant to shear banding is convective constraint release (CCR), which enables the relaxation of some stress carried by the test chain due to the reconfiguration of the tube when an entanglement point is lost as chains slide past each other. Such CCR becomes increasingly important with the shear rate and was shown to be able to remove the nonmonotonicity of the original tube model. We note that arguments were put forth to justify a lesser degree of CCR in wormlike micelles (owing to breaking/recombination) and thus allow the existence of shear banding in micelles (Milner et al. 2001). These arguments were shown to be correct in very recent simulations (Zou & Larson 2014).

Since 2006, strong efforts have been made to provide a 1D picture using velocimetry techniques in various flow geometries, mostly CP (Ravindranath et al. 2008, Li et al. 2013) and parallel plate (Boukany & Wang 2007, Hayes et al. 2008) and marginally TC (Hu 2010) and pipe (Zhu et al. 2013). During the past decade, extensive sets of particle tracking velocimetry (PTV) experiments combined with global rheology by Wang et al. (2011) showed that shear banding can emerge in polymer solutions and melts (**Figure 3a**). Recently, shear banding in polymers has also been evidenced by other groups using optical coherence tomography (Jaradat et al. 2012) or PTV (Noirez et al. 2009). As in wormlike micelles, shear banding was often found to compete with wall slip (Boukany & Wang 2008, Jaradat et al. 2012), which seems ubiquitous in these systems and can be limited by surface roughness or the treatment and use of entangled polymeric solvent. The

Figure 2

(a) 2D picture of shear-banding flow in semidilute wormlike micelles, illustrating evidence for elastic instability and turbulence in Taylor-Couette flow. (i) Steady-state velocity map $v_\theta(r, z)$ deduced from ultrasonic imaging for a given shear rate. The maps on the right are magnifications showing the radial $v_r(r, z)$ and azimuthal $v_\theta(r, z)$ velocity components, respectively. (ii,iii) Views of the gap in the (r, z) plane illuminated with either white light or laser light, the former providing direct visualization of the vortex structure responsible for the undulation of the interface. The gap size (1.13 mm) corresponds to the width of the picture, and the bar (1 mm) gives the vertical scale. In parts *i* and *ii*, the system is made of cetyltrimethylammonium bromide and sodium nitrate, and part *iii* shows a sample of cetylpyridinium chloride with sodium salicylate in brine for different applied shear rates. Panel *a* adapted with permission from Fardin & Lerouge (2014), copyright by the Royal Society of Chemistry. (b) 1D picture of shear-banding flow in semidilute wormlike micelles. (i) Flow birefringence snapshot in the (r, θ) plane. The annular gap is illuminated with white light and placed between crossed polarizers. The evidence of three bands is purely artifactual. The intermediate band results from the interfacial undulation and leads to smooth orientation profiles between bands. Part *i* of panel *b* adapted with permission from Lerouge et al. (2004), copyright by the American Chemical Society. (ii) Time-averaged velocity profiles for different applied shear rates associated with the images in part *iii* of panel *a*. (iii) Selection of several instantaneous velocity profiles, illustrating the impact of a turbulent burst on the main flow. Parts *ii* and *iii* of panel *b* adapted with permission from Fardin et al. (2012c), copyright by the Royal Society of Chemistry.

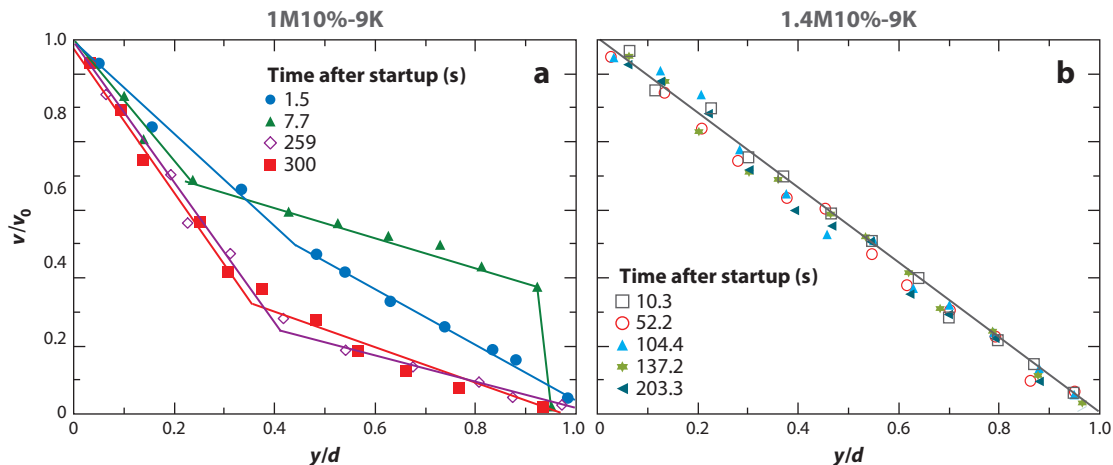


Figure 3

Velocity profiles at different times following the start-up of flow and gathered in rotating parallel plate geometry. d is the gap size, and v_0 is the velocity of the moving plate at the radius where local velocities are measured. (a) The sample is a polybutadiene solution (1M10%-9K) with an entanglement density $Z = 42$. Panel a adapted with permission from Ravindranath et al. (2008), copyright by the American Chemical Society. (b) The sample is a polybutadiene solution (1.4M10%-9K) with an entanglement density $Z = 55$. Panel b adapted with permission from Li et al. (2013), copyright by the Society of Rheology.

emergence of shear banding in polymer solutions and melts seems to require sufficiently entangled (Boukany & Wang 2009b) and monodisperse (Boukany & Wang 2007) samples. Furthermore, the competition between shear banding and wall slip seems to depend on both the concentration and molecular weight (Wang et al. 2011, Jaradat et al. 2012), and bulk banded flows are likely to overcome slip effects for sufficiently high applied shear rates (Boukany & Wang 2008, 2009a). Finally, the existence of steady shear banding seems to be connected to the flow history, at least for solutions (Boukany & Wang 2010, Cheng & Wang 2012). Indeed, shear banding seems to be observed at steady state following start-up shear protocols, and it seems to be a transient property when using shear ramp protocols.

However, up to now, the 1D picture described above has not reached a consensus. PTV experiments in TC flow showing the possible existence of both banded and nonbanded profiles for a given sample in the supposed regime of shear banding suggested that shear banding may be only a long-lived transient feature in polymer solutions (Hu 2010). In contrast, other groups observed neither transient nor steady shear banding (Hayes et al. 2008, 2010; Li et al. 2013) (Figure 3b). They concluded that wall slip and linear velocity profiles prevail in the response of polymer solutions. In addition, it was suggested that edge effects or experimental artifacts may be responsible for the observed shear banding in polymer solutions (Li et al. 2013, 2014).

This situation gave rise to impassioned debates (Adams & Olmsted 2009a,b; Wang 2009). Wang's interpretation of shear banding involves microscopic failure occurring within the bulk under large step shear, thus challenging the tube picture, which cannot account for such elastic yielding. Hence, rejecting almost the entire reptation picture on one side, and casting doubt on the quality of experiments on the other, the controversy on shear banding in polymers is far from being sorted out (Wang et al. 2014, Li et al. 2014). Nonetheless, it stimulated much theoretical work trying to provide rationales for the various experimental observations, as illustrated in the next section.

2.3. Theoretical Frameworks for Shear Banding in Polymeric Fluids

As mentioned above, the tube-like models with all their modern additions can predict shear banding in entangled polymeric fluids (Milner et al. 2001) and wormlike micelles (Cates & Fielding 2006). However, these microscopic models are not always easily tractable in the nonlinear flow regime. In practice, more phenomenological models are used instead (Cates & Fielding 2006, Olmsted 2008). These models do not usually contain all the information on the dynamics of the microstructure and deal with coarse-grained quantities defined at the macroscopic scale. They usually at least include tensorial stress and velocity gradient fields. Simple phenomenological models such as the diffuse Johnson-Segalman model and the diffusive Giesekus model can qualitatively reproduce many of the macroscopic aspects of shear banding. Nonetheless, they are too coarse grained to differentiate between micelles and polymers. A compromise between microscopic and phenomenological models is the so-called Rolie-Poly model, which is a simplified differential version of the tube model that incorporates CCR.

Phenomenological models of shear banding in polymeric fluids usually rely on a disjunction of the stress into two parts: a solvent part ($\eta_{\text{sol}}\dot{\gamma}$), and a polymer part ($\eta_{\text{pol}}\dot{\gamma}$). The polymer part, like in the tube models, increases only up to a critical shear rate, after which it continuously decreases. Ultimately, the viscosity at an infinite shear rate is η_{sol} . Shear banding emerges if the so-called viscosity ratio ($\eta \equiv \eta_{\text{sol}}/\eta_{\text{pol}}$) is small enough for the total flow curve to be nonmonotonic. This behavior is also observed experimentally in wormlike micelles, by varying the concentration in surfactant or the temperature (**Figure 1b**). Above a critical viscosity ratio, η_c , steady shear banding disappears. Furthermore, nonlocal (diffusive) terms have been included in the equation governing the polymeric stress to account for experimental observations in wormlike micelles of a unique stress plateau at σ_p independent of the shear history and the initial conditions (see Olmsted 2008 for a review). Such diffusion terms are now widespread and allow one to define the typical width of the interface between bands as a function of the stress diffusion coefficient, $\ell \equiv \sqrt{D\tau_e}$, where τ_e is the relaxation time of the fluid. During the past decade, phenomenological models including diffusive terms were used to test the impact of the flow geometry (Radulescu & Olmsted 1999) and the boundary conditions (Adams et al. 2008) on the banding structure, the role of flow-concentration coupling (Fielding & Olmsted 2003), the effect of the control parameter (Dhont 1999), and more recently the stability of the shear-banding flow (Fielding 2010, Nicolas & Morozov 2012).

In tube models and in the more phenomenological models such as the diffuse Johnson-Segalman model, the shear-banding instability is seen from the mechanical perspective we mostly echo above. Shear banding in wormlike micelles can also be approached from a more thermodynamic perspective, noting the similarities between shear banding and first-order phase transitions. For instance, the critical viscosity ratio η_c leads to a flow curve with an inflection point that shares much similarity with a critical point. Unfortunately, this critical point has remained largely unexplored experimentally. Generally, **Figure 1b** can be called a flow-phase diagram. If the thermodynamic and mechanical perspectives were once competing, they are now understood as two sides of the same coin. Even if the rationale for shear banding provided by the tube picture for polymeric fluids seems to be the correct one, other possibilities are nonetheless investigated.

In particular, in wormlike micelles, the Vasquez-Cook-McKinley model has been shown to be able to reproduce many of the properties of shear banding observed in experiments (Zhou et al. 2014). This model, devised at the intermediate level of kinetic theories, is built out of two species of dumbbells, short and long, for which two short ones are allowed to combine into a long one, and long ones increasingly break apart as the flow strength is increased. In effect, shear banding in this model is a consequence of shear-induced demixing of long and short species, with long ones eventually disappearing entirely. This explanation for shear banding differs from the one

provided by tube models, and whether it applies to shear banding in wormlike micelles should be checked experimentally by investigating if the typical length of micelles at a high shear rate is indeed shorter than that at a low shear rate.

Finally, we return to the controversial situation in polymer solutions and melts. Using the diffusive Rolie-Poly model, Adams, Olmsted, and colleagues first highlighted that transient shear banding could appear in polymeric flows for viscosity ratios η just above the critical value η_c (i.e., for flow curves that are actually monotonic or equivalently for nonbanded steady states) (Adams & Olmsted 2009a, Adams et al. 2011). Key ingredients for the emergence of transient shear banding are thermal noise or high stress gradients inherent to the flow geometry. This observation was subsequently extended by Moorcroft, Fielding, and colleagues, who derived a very general mechanical criterion encompassing all complex fluids to predict the occurrence of transient as well as steady shear banding (Moorcroft et al. 2011, Moorcroft & Fielding 2013). Checking the validity of this criterion for wormlike micellar solutions with a viscosity ratio above and below the limit η_c appears to be a logical next step for experiments. The diffusive Rolie-Poly model was also recently used to offer further ways to interpret the data on shear banding in polymers (Agimelen & Olmsted 2013). Recently, another alternative involving the Rolie-Poly model was also shown to qualitatively reproduce almost all the phenomena observed by Wang's group for a model polymer solution with an underlying monotonic constitutive curve, with the driving mechanism being the coupling of the polymer stress to an inhomogeneous concentration profile (Cromer et al. 2014).

3. SHEAR BANDING IN SOFT GLASSY MATERIALS

Having reviewed the current state of knowledge on shear banding in polymeric solutions, we now discuss shear banding in soft glassy materials (SGM). Here we use the term glassy in a broader sense than generally assumed, by encompassing complex fluids that can be either liquid-like or solid-like at rest but that are all characterized by a microstructure in which elementary bricks strongly interact (e.g., through steric constraints, entanglements, attractive forces, or physical bonds). On the one hand, liquid-like SGM correspond to solutions of surfactants or copolymers, yet at higher concentrations than the wormlike systems discussed above. These solutions display highly viscoelastic lyotropic mesophases, such as hexagonal, lamellar, cubic, and bicontinuous sponge phases. On the other hand, solid-like SGM are systems in which microconstituents are kinetically trapped into a disordered, metastable configuration and thermal energy alone is not sufficient to significantly rearrange the microstructure and relax mechanical stresses. The glassy behavior of such SGM originates from either geometric frustration or attractive interactions between the constituents, and they typically exhibit a yield stress; that is, they can rearrange and flow provided a stress larger than some critical value σ_c is applied. Examples of solid-like SGM range from concentrated jammed systems of repulsive hard spheres, soft particles, or liquid droplets to dispersions of attractive colloids that form space-spanning networks even at very low volume fractions (i.e., colloidal gels).

There is currently no universal explanation for heterogeneous flows in SGM, and in comparison to wormlike micellar fluids, the picture is at best fragmented, if not controversial. Clearly, difficulties in characterizing and understanding shear banding in SGM arise from the fact that, as the zero-shear viscosity increases and eventually goes to infinity upon jamming or gelation, relaxation times considerably increase so that at least one of the characteristic shear rates $\dot{\gamma}_1$ and $\dot{\gamma}_2$ apparently goes to zero, as sketched in **Figure 4**. In particular, to be conclusive, any study involving low shear rates or focusing on solid–fluid coexistence must be performed over long-enough timescales to ascertain that a steady state is reached. Over the years, it has progressively

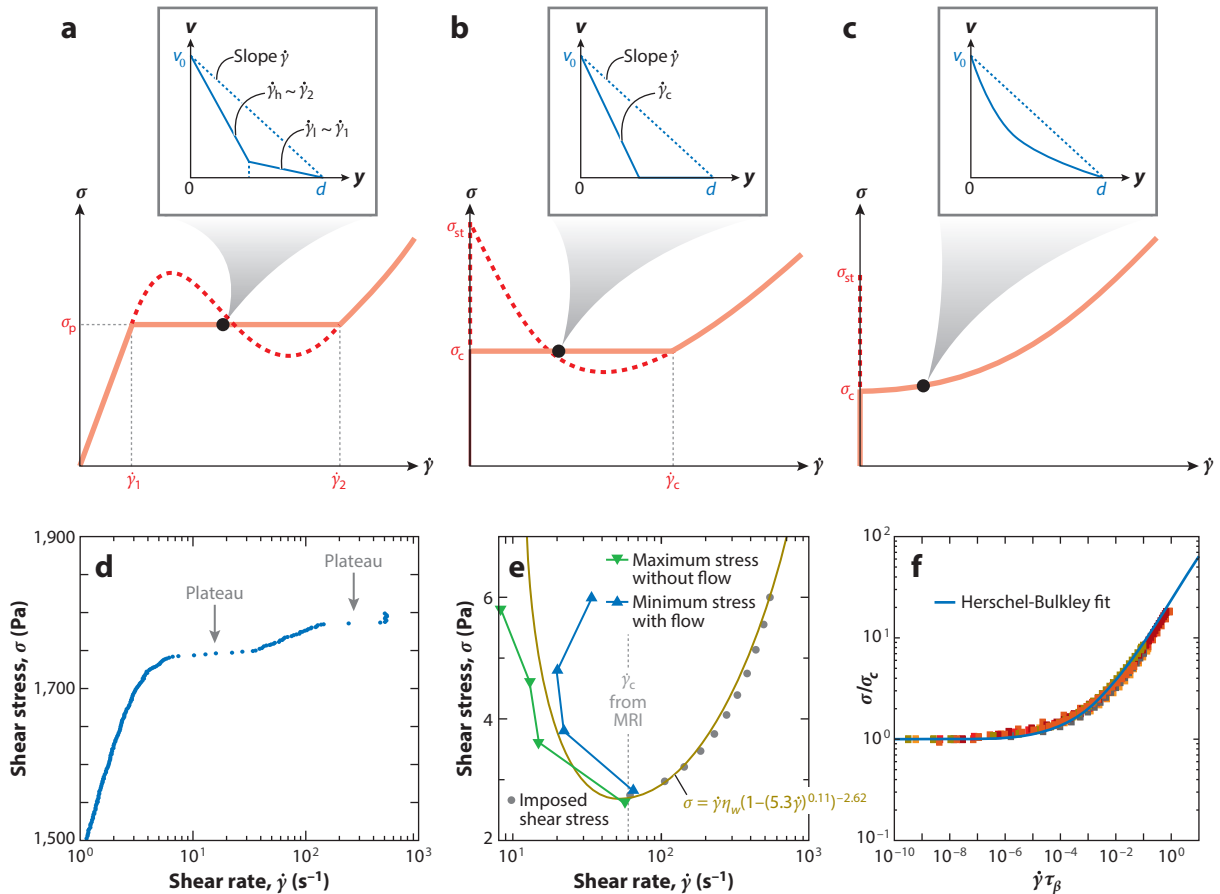


Figure 4

Sketches of the flow curves σ versus $\dot{\gamma}$ and the velocity profiles $v(y)$ expected in (a) materials undergoing a mechanical instability or a shear-induced transition, such as semidilute wormlike micellar solutions or lamellar and cubic phases; (b) a yield stress material with steady-state shear banding below a critical shear rate $\dot{\gamma}_c$; and (c) a yield stress material that follows a Herschel-Bulkley rheology and flows homogeneously in the steady state. σ_p stands for the value of the stress plateau in panel a, and σ_c and σ_{st} denote the apparent yield stress and the static yield stress, respectively, in panels b and c. In the sketched velocity profiles, the blue dotted lines indicate the case of a Newtonian fluid. v_0 stands for the velocity of the moving wall. These three different types of flow curves are illustrated for (d) a cubic phase of a triblock copolymer made of ethylene and propylene oxide, showing two successive stress plateaus; (e) a colloidal suspension of Ludox silica spheres; and (f) microgels with different cross-link densities made of acrylate chains bearing methacrylic acid units. In panel f, σ has been rescaled by the yield stress σ_c , and $\dot{\gamma}$ has been rescaled by the inverse of the fluid microstructural relaxation time inferred from light-scattering experiments τ_β . The continuous line is the best Herschel-Bulkley fit. Panels d–f adapted with permission from Eiser et al. (2000a), Møller et al. (2008), and Cloitre et al. (2003), respectively, copyright by the American Physical Society. Abbreviation: MRI, magnetic resonance imaging.

been recognized that, depending on the nature of the fluid microstructure and on the interactions between its constituents, shear banding in SGM originates from one or a combination of the following causes: (a) an underlying shear-induced phase transition, (b) the competition between shear and the attractive interactions between the constituents, or (c) flow–concentration coupling. For instance, a dilute assembly of monodisperse colloidal hard spheres may develop a shear band owing to flow-induced crystallization (Shereda et al. 2010), whereas more concentrated and slightly

polydisperse samples may experience the formation of a permanently arrested band because of minute variations of the local packing fraction that trigger the jamming of a macroscopic region of the flow (Besseling et al. 2010).

In what follows, we have chosen to deepen the phenomenology of shear banding in SGM through a historical approach put into perspective by recent progress in modeling. We first discuss the case of concentrated surfactants and block copolymers, for which shear banding mainly results from shear-induced structuration, before turning to colloidal star polymers that display a delayed scenario for shear band formation. SGM with a yield stress are the topic of the Sections 3.2 and 3.3, where we review steady-state shear banding, the most studied case so far, and transient shear banding, an emerging area in SGM, respectively.

3.1. From Shear-Thinning Fluids to Glassy, Yet Not Jammed Materials

Concentrated surfactants and block copolymers exhibit lyotropic mesostructures whose properties under shear have been the topic of numerous studies. Close to an equilibrium phase transition, shear may indeed help the system cross the phase boundary. Sheared liquid crystalline phases may also organize to form novel out-of-equilibrium shear-induced structures and are likely to involve shear banding (Berni et al. 2002). Under moderate shear, some lamellar phases were shown to organize into a novel structure of disordered close-compact multilamellar vesicles called onions (Diat et al. 1993). This disordered onion assembly itself undergoes a shear-thinning transition at larger shear at which the final state is characterized by hexagonally ordered onion layers sliding on top of each other along the velocity direction (Roux et al. 1993). In the vicinity of this layering transition, velocimetry revealed that the nucleation and growth of such shear-induced structures are associated with the nucleation and growth of a shear band, and that the classical picture of shear banding detailed in Section 2.1, including the lever rule, holds true (Salmon et al. 2003b). However, numerical simulations of lamellar systems that reproduce shear banding show no evidence of a stress plateau, which suggests that if the shear band is robust, the lever rule may not be universal in these systems (Xu et al. 2006).

A quite similar situation has been reported in concentrated copolymer solutions forming spherical micelles that arrange into cubic phases. Under shear, the initial disordered polycrystalline structure successively orients into different bcc crystals, each transition being signaled by a stress plateau (**Figure 4d**) at which two structures coexist, as evidenced by X-ray diffraction (Eiser et al. 2000a; for a review of the shear-induced states in block copolymers, see Hamley 2001). We also note that such orientation transitions are reminiscent of those observed in colloidal crystals (Chen et al. 1994). Whereas block copolymers forming wormlike micellar structures have been shown to display shear banding and elastic instabilities reminiscent of surfactant wormlike systems (Manneville et al. 2007), the local flow properties of more concentrated copolymers remain largely unexplored and deserve more attention in future studies to fully understand these shear-induced transitions (Eiser et al. 2000b). Another line of research concerns so-called transient networks comprising, for example, reversibly cross-linked telechelic copolymers or proteins (see Ligoure & Mora 2013 for a review). Although these systems have long been known to fracture under shear, a phenomenon associated with a decrease of the stress with strain (Skrzeszewska et al. 2010), the shear banding recently reported in a numerical model of a transient network (Billen et al. 2015) raises the fundamental question of whether fractures could be seen as an extreme case of shear bands.

Finally, dense suspensions of hairy soft particles made of colloidal star polymers display rheological properties that are intermediate between the above systems and the concentrated colloids addressed in Section 3.2 (Christopoulou et al. 2009, Vlassopoulos & Fytas 2010). They

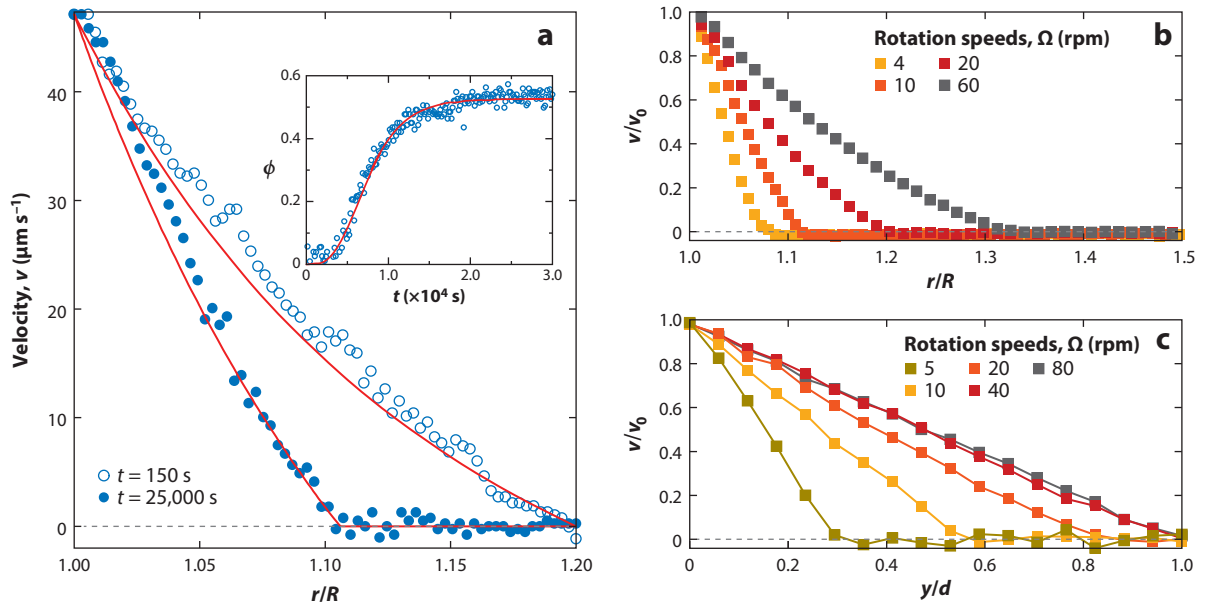


Figure 5

(a) Velocity profiles at different times, $t = 150$ s (open blue circles) and $t = 25,000$ s (filled blue circles), during a shear start-up experiment ($\dot{\gamma} = 3.14 \times 10^{-2} \text{ s}^{-1}$) for a system of colloidal star polymers sheared in a wide-gap Taylor-Couette geometry of inner radius $R = 7.5$ mm and gap size $d = 1.5$ mm. The red curves correspond to the predictions of a fluidity model. (Inset) Temporal evolution of the fraction ϕ of jammed material in the gap, fitted by an exponential function (red line). Panel a adapted with permission from Rogers et al. (2008), copyright by the American Physical Society. (b) Normalized steady-state velocity profiles in a drilling mud in a wide-gap cone-and-plate geometry ($R = 40$ mm, $d = 20$ mm) at different rotation speeds. Panel b adapted with permission from Ragouilliaux et al. (2006), copyright by Springer-Verlag. (c) Normalized steady-state velocity profiles in a cone-and-plate geometry for a bentonite suspension at different rotation speeds. y denotes the vertical position within the cone, and d stands for the gap thickness ($d = 4.7$ mm at the periphery of the cone). Panel c adapted with permission from Ovarlez et al. (2009), copyright by Springer-Verlag.

are liquid-like and shear thinning at short times after the application of an oscillatory preshear but strikingly develop shear-banded velocity profiles over thousands of seconds (Figure 5a) (Rogers et al. 2008). Such delayed transients toward a heterogeneous steady state are observed below a critical shear rate $\dot{\gamma}_c$ that depends on the particle concentration (Holmes et al. 2004, Rogers et al. 2010). The slow emergence of a yield stress and of a stress plateau spanning from 0 to $\dot{\gamma}_c$ in the flow curve of colloidal star polymer suspensions has been attributed to the progressive entanglement of percolating groups of particles (Rogers et al. 2010), and similar long-lived transients have been reproduced in Brownian dynamics simulations (van der Noort & Briels 2008). Such time dependence, or aging, is also key to the formation of steady heterogeneous flows, as we also see below for SGM comprising attractive colloidal particles.

3.2. Steady-State Shear Banding in Yield Stress Fluids

In the early 1990s, shear banding in yield stress fluids (YSF) was originally referred to as shear localization and denoted the coexistence of two (or more) partially sheared bands, often sliding along each other, during transient or steady-state flows. These heterogeneous flows had been identified thanks to seminal experiments conducted on complex materials often inherited from industry (e.g., ink, lubricating grease) in parallel plate and TC geometries. In pioneering work,

Piau and coworkers unveiled a wide range of heterogeneous flows in clay suspensions and Carbopol microgels, including fractures, wall slip, the coexistence of plug flow(s) or shear band(s), and stick-slip dynamics, by simply following a line painted along the vorticity direction at the sample periphery (Magnin & Piau 1990, Pignon et al. 1996). To rationalize such a wealth of flows, experimentalists quickly focused on two other geometries that made flow visualization easier and more quantitative, namely TC geometry and channel flow. Coupled to local techniques such as light scattering, particle tracking, magnetic resonance, ultrasonic echography, and confocal microscopy, rheological tests were much enriched by the simultaneous measurement of bulk velocity fields (Callaghan 2008, Manneville 2008). Historically, experiments in wide-gap TC cells have played a particular role in the understanding of shear banding. We recall that in TC geometry the local shear stress decreases from the inner to the outer cylinder as $1/r^2$, where $r = R + y$ denotes the distance to the rotation axis. Therefore, shear banding is somewhat trivially observed when the yield stress of the fluid under scrutiny lies between the maximum and minimum local stresses. Of course, this situation also occurs in any channel flow as soon as the wall shear stress exceeds the yield stress, as the local stress always vanishes at the center of the channel. Such shear banding induced solely by the stress heterogeneity inherent to the geometry is now referred to as shear localization to make a clear distinction with the intrinsic shear banding related to the nonlinear rheology of the material (Ovarlez et al. 2009), toward which we now turn.


Interestingly, numerous YSF with strong attractive interactions display steady-state heterogeneous velocity profiles that cannot be attributed to the shearing geometry. The coexistence between a flowing band and a solid-like region rather results from the existence of a critical shear rate $\dot{\gamma}_c$ below which no steady homogeneous flow is possible (Coussot et al. 2002a,b). In terms of the flow curve, this corresponds to the case of wormlike micelles explored in Section 2, but the lower characteristic shear rate $\dot{\gamma}_1$ would be set to zero, and the upper limit of the stress plateau $\dot{\gamma}_2$ would correspond to $\dot{\gamma}_c$. This analogy (**Figure 4b,e**) has been quantitatively pushed forward thanks to experiments performed on attractive colloids in CP geometry (Coussot et al. 2002b, Møller et al. 2008, Ovarlez et al. 2009). For a homogeneous shear rate $0 \leq \dot{\gamma} \leq \dot{\gamma}_c$, steady-state shear banding was observed with a flowing band sheared at $\dot{\gamma}_c$ over a width roughly following the lever rule, with $\dot{\gamma}_1 = 0$ and $\dot{\gamma}_2 = \dot{\gamma}_c$ (**Figure 5b,c**). However, the situation is far less clear than that for wormlike micelles as there is a lack of measurements on other systems, and the chemical and physical nature of the boundary conditions as well as the preshear protocol prior to the experiment may strongly influence the results (Gibaud et al. 2008, Cheddadi et al. 2012). Last but not least, despite the formal analogy with wormlike micelles, the physical origin of the characteristic timescale $\dot{\gamma}_c^{-1}$ remains an open issue.

From a theoretical perspective, the very existence of $\dot{\gamma}_c$ is still highly debated, even though it quickly emerged naturally from toy models based on the competition between shear and spontaneous physical aging (Møller et al. 2006, Coussot & Ovarlez 2010). The prevailing picture somewhat differs from the interpretation of nonmonotonic flow curves in terms of a mechanical instability. It rather builds on the generic observation that the static yield stress σ_{st} above which the system starts flowing from the solid state is larger than the dynamic yield stress (i.e., the minimal stress at which the material is observed to flow when the shear rate is decreased from large values) (Picard et al. 2002). The flow curve can thus be seen as the superposition of a monotonic flow curve pointing toward the dynamic yield stress for vanishing shear rates, and of a static branch at $\dot{\gamma} = 0$, for stresses below the static yield stress (**Figure 4c**). This scenario, which does not necessarily imply the presence of an underlying decreasing flow curve below some critical $\dot{\gamma}_c$, is supported by simulations of Lennard-Jones glasses (Varnik et al. 2003, Tsamados 2010) and by numerical work on concentrated soft particles (Chaudhuri et al. 2012).

In this framework, the key role of attractive interactions has been mainly illustrated using emulsions made adhesive either by depletion forces (Bécu et al. 2006) or by the minute addition of clay particles bridging the droplets (Ragouilliaux et al. 2007, Paredes et al. 2011). Recent numerical simulations of athermal assemblies of soft particles show that adding attraction to a system slightly below jamming leads to a nonmonotonic flow curve and to steady-state shear banding (Irani et al. 2014). However, experimentally, the question of whether there is a minimal amount of attraction required to generate steady-state shear banding remains open. Similarly, quantitative details on the potential link between the interaction potential and the critical shear rate $\dot{\gamma}_c$ are still lacking.

3.3. From Steady-State to Transient Heterogeneous Flows

Not all solid-like SGM display steady-state heterogeneous flows. Shear banding may be only transient and give way to a homogeneously sheared flow after long-lived induction periods. Such delayed, heterogeneous fluidization, now referred to as transient shear banding, has been reported for a large range of shear stresses above the yield stress on Carbopol microgels (Divoux et al. 2010, 2011) (see **Supplemental Video 1**; follow the **Supplemental Material link** from the Annual Reviews home page at <http://www.annualreviews.org>), carbon black gels (Gibaud et al. 2010, 2014), and Laponite clay suspensions (Gibaud et al. 2008, Martin & Hu 2012). The corresponding time-resolved scenario broadly involves several successive steps: homogeneous elastic deformation, strong (if not complete) slippage at the walls, and nucleation and growth of a shear band that eventually spans the whole sample at a well-defined full fluidization time τ_f that dramatically increases in the vicinity of the yield stress (Gibaud et al. 2009, Divoux et al. 2012) (**Figure 6a,b**). In particular, it has been established that τ_f diverges as power laws $\tau_f(\sigma) \propto 1/(\sigma - \sigma_c)^\beta$ and $\tau_f(\dot{\gamma}) \propto 1/\dot{\gamma}^\alpha$ in Carbopol microgels (Divoux et al. 2010, 2011) (**Figure 6c**). Remarkably, in this system, in which steady-state rheology follows the mostly phenomenological Herschel-Bulkley scaling $\sigma = \sigma_c + A\dot{\gamma}^n$ (**Figure 4f**), it could be shown that the exponent n is linked to those of transient shear banding through $n = \alpha/\beta$. Such results strongly support interpretations in terms of critical phenomena and dynamical phase transitions (Bocquet et al. 2009, Divoux et al. 2012, Chikkadi et al. 2014).

 Supplemental Material

However, a general picture on transient shear banding is still out of reach and certainly depends on the microscopic details of the system. For instance, in spite of similar dynamics, τ_f in weakly attractive colloidal gels does not follow critical-like power laws but rather obeys exponential Arrhenius-like scalings (**Figure 6d**), hinting at a central role played by thermally activated processes (Gopalakrishnan & Zukoski 2007, Gibaud et al. 2010, Sprakel et al. 2011, Grenard et al. 2014). Still, the microscopic ingredients at the origin of exponential versus power-law scalings involved in such delayed yielding remain to be uncovered, and predicting transient flow dynamics from microstructural information is an important open research topic (Chaudhuri & Horbach 2013).

Despite these difficulties, a general criterion for transient banding has been recently formulated by Fielding (2014) in the framework of trap and fluidity models. Both approaches rely on the strong viscoelastic responses of YSF and predict the formation of transient heterogeneous flows during the stress relaxation that follows the stress overshoot observed after shear start-up (Moorcroft & Fielding 2013). This approach is further supported by recent experiments on Laponite suspensions (Martin & Hu 2012).

4. CONCLUSION

In fluid dynamics and in continuum approaches in general, the formalism is set up in such a way as to start from states that are usually assumed to be homogeneous and laminar, steady, and stable.

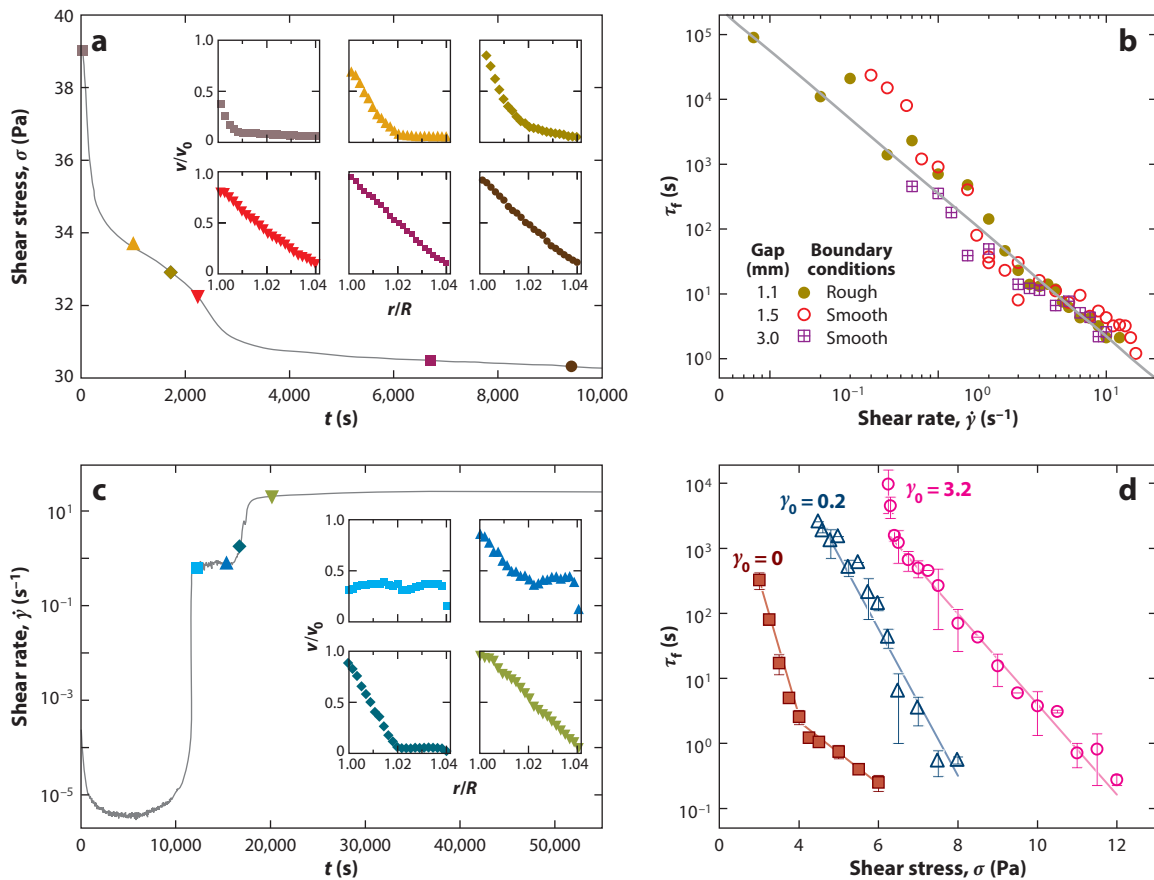


Figure 6

(a) Stress response $\sigma(t)$ of a Carbopol microgel to a shear start-up experiment at $\dot{\gamma} = 0.7 \text{ s}^{-1}$ in a small-gap Taylor-Couette (TC) geometry with $R = 23.9 \text{ mm}$ and $d = 1.1 \text{ mm}$ (see **Supplemental Video 1**). (Insets) Normalized velocity profiles v/v_0 at different times. The corresponding times are indicated in the main panel using the same symbols. (b) Fluidization time τ_f versus the applied shear rate $\dot{\gamma}$ for various gap widths and boundary conditions. The gray line is the best power-law fit with an exponent $\alpha = 2.3 \pm 0.1$. Panels *a* and *b* adapted with permission from Divoux et al. (2010), copyright by the American Physical Society. (c) Shear rate response $\dot{\gamma}(t)$ during a creep experiment in a 10 wt% carbon black gel at $\sigma = 55 \text{ Pa}$ in a sand-blasted small-gap TC cell of inner radius $R = 24 \text{ mm}$ and $d = 1 \text{ mm}$. (Insets) Normalized velocity profiles v/v_0 at different times. The corresponding times are indicated in the main panel using the same symbols. Panel *c* adapted with permission from Grenard et al. (2014), copyright by the Royal Society of Chemistry. (d) Fluidization time τ_f versus the applied stress σ for a thermoreversible gel of stearylated silica particles. The different curves correspond to gels that have been prepared by applying different levels of strain γ_0 prior to each creep experiment. The lines correspond to exponential fits. Panel *d* adapted with permission from Sprakel et al. (2011), copyright by the American Physical Society.

Supplemental Material

Nevertheless, time and time again, experiments have shown that as soon as sufficient power is delivered into the material (e.g., by applying shear), inhomogeneity, instabilities, and transient or intermittent effects creep into the flow fields (e.g., velocity field, deformation rate field, stress field, concentration field). For example, viscoelasticity, yielding, flow instabilities, turbulence, flow-induced structures, shear banding, and other types of shear localization all show us various aspects of a common fate. In this review, we have tried to isolate shear banding by laying out some of its salient properties across complex fluids. One such property is that it can be understood to a good extent by referring only to the mechanical fields of stress versus the shear rate: It can be

understood as a material instability. But as in any nonlinear context, identifying the cause from the effect is not always trivial. Nonmonotonic flow curves and shear banding seem quite tightly connected, but they are not equivalent. Is shear banding causing the nonmonotonic flow curve, or is the nonmonotonic flow curve causing shear banding? In some cases, the answer is not so clear-cut, as wall slip, structural changes, concentration differences, or flow instabilities can also be at play.

In the case of polymeric fluids, research on solutions of wormlike micelles provides a road map on how to disentangle some of the nonlinear effects from each other. Nevertheless, much research remains ahead, and the controversial status of shear banding in polymers is a testimony to this state of affairs. Even the spurt effect that motivated the use of the term shear banding in fluids remains an open issue. Shear banding, wall slip, and flow instabilities may all have some effects on this phenomenon.

As for SGM, the presence of attractive interactions between the constituents, either controlled by van der Waals forces or produced by long-lived sticky contacts between the particles, leads to a rich and complex phenomenology in which aging and time dependence play a major role. Shear banding in attractive SGM intrinsically depends on the initial state and on the shear history, as well as on the nature of the boundary conditions.

In both polymeric materials and SGM, wall slip can no longer be described as a mere rheological artifact decoupled from bulk rheology (Barnes 1995, Buscall 2010). For instance, space- and time-resolved studies have indeed shown that slippery walls foster fluidization against steady-state shear banding (Gibaud et al. 2009). The chemical nature of the walls also modifies the flow profiles far away from the boundaries (Seth et al. 2012). Such a strong influence of boundary conditions on both transient and steady-state flows is not yet captured by models, and we believe that a major theoretical challenge for future years is to include the effects of boundaries at least through coarse-grained approaches, if not at the microscopic level.

More generally, the question of whether shear banding in polymeric systems and that in SGM are of similar fundamental nature remains open. Strikingly, various models, such as fluidity models, seem to apply equally well to both kinds of systems and, up to minor adaptations, have been able to reproduce subtle effects of confinement on shear banding (Goyon et al. 2008, Masselon et al. 2008), as well as transient regimes in polymeric and glassy systems (Fielding 2014). Although devising a general theory from a first-principles approach independently of the system details is probably not a realistic challenge, the solid-fluid coexistence in SGM may be fundamentally not so far from the coexistence of flowing bands in polymeric fluids.

FUTURE ISSUES

1. Can shear banding in polymeric materials and SGM be understood within the same framework? The mechanical criterion proposed by Moorcroft and Fielding provides a promising approach, which remains to be fully tested in experiments.
2. More microscopically, what are the relevant parameters (e.g., interaction potential, relaxation mechanisms) that generate the critical shear rates for shear banding ($\dot{\gamma}_1$, $\dot{\gamma}_2$, or $\dot{\gamma}_c$) and the value of the stress plateau?
3. In both polymeric materials and SGM, wall slip seems quite tightly connected to shear banding. How could this be incorporated systematically into theoretical models? More generally, how do the chemistry and the deformability of the boundary conditions impact the fluid dynamics, especially during transient flows?

4. What is the extent of the interplay between shear banding and elastic instabilities and/or concentration fluctuations?

DISCLOSURE STATEMENT

The authors are not aware of any biases that might be perceived as affecting the objectivity of this review.

ACKNOWLEDGMENTS

The authors acknowledge funding from the European Research Council under the European Union's Seventh Framework Program (FP7/2007–2013)/ERC grant agreement 258803, from Institut Universitaire de France and from the CNRS “Theoretical Physics and Interfaces” PEPS project “ComplexWall.” We thank P. Coussot, S. Lindström, and D. Vlassopoulos for kindly providing us with their original data.

LITERATURE CITED

- Adams JM, Fielding SM, Olmsted PD. 2008. The interplay between boundary conditions and flow geometries in shear banding: hysteresis, band configurations, and surface transitions. *J. Non-Newton. Fluid Mech.* 151:101–18
- Adams JM, Fielding SM, Olmsted PD. 2011. Transient shear banding in entangled polymers: a study using the Rolie-Poly model. *J. Rheol.* 55:1007–32
- Adams JM, Olmsted PD. 2009a. Nonmonotonic models are not necessary to obtain shear banding phenomena in entangled polymer solutions. *Phys. Rev. Lett.* 102:067801
- Adams JM, Olmsted PD. 2009b. Adams and Olmsted reply. *Phys. Rev. Lett.* 103:219802
- Agimelen OS, Olmsted PD. 2013. Apparent fracture in polymeric fluids under step shear. *Phys. Rev. Lett.* 110:204503
- Ballesta P, Lettinga MP, Manneville S. 2007. Superposition rheology of shear-banding wormlike micelles. *J. Rheol.* 51:1047–72
- Barnes HA. 1995. A review of the slip (wall depletion) of polymer solutions, emulsions and particle suspensions in viscometers: its cause, character, and cure. *J. Non-Newton. Fluid Mech.* 56:221–51
- Bécu L, Anache D, Manneville S, Colin A. 2007. Evidence for three-dimensional unstable flows in shear-banding wormlike micelles. *Phys. Rev. E* 76:011503
- Bécu L, Manneville S, Colin A. 2006. Yielding and flow in adhesive and nonadhesive concentrated emulsions. *Phys. Rev. Lett.* 96:138302
- Bercea M, Peiti C, Simionescu B, Navard P. 1993. Shear rheology of semidilute poly (methyl methacrylate) solutions. *Macromolecules* 26:7095–96
- Berni M, Lawrence C, Machin D. 2002. A review of the rheology of the lamellar phase in surfactant systems. *Adv. Colloid Interface Sci.* 98:217–43
- Berret J. 2006. Rheology of wormlike micelles: equilibrium properties and shear banding transitions. In *Molecular Gels*, ed. RG Weiss, P Terech, pp. 667–720. New York: Springer
- Besseling R, Ballesta LIP, Petekidis G, Cates M, Poon W. 2010. Shear banding and flow-concentration coupling in colloidal glasses. *Phys. Rev. Lett.* 105:268301
- Billen J, Wilson M, Baljon A. 2015. Shear banding in simulated telechelic polymers. *Cbem. Phys.* 446:7–12
- Bird R, Armstrong R, Hassager O. 1987. *Dynamics of Polymeric Liquids*, Vol. 1: *Fluid Mechanics*. New York: Wiley
- Bocquet L, Colin A, Ajdari A. 2009. A kinetic theory of plastic flow in soft glassy materials. *Phys. Rev. Lett.* 103:036001

- Boukany PE, Wang SQ. 2007. A correlation between velocity profile and molecular weight distribution in sheared entangled polymer solutions. *J. Rheol.* 51:217–33
- Boukany PE, Wang SQ. 2008. Use of particle-tracking velocimetry and flow birefringence to study nonlinear flow behavior of entangled wormlike micellar solution: from wall slip, bulk disentanglement to chain scission. *Macromolecules* 41:1455–64
- Boukany PE, Wang SQ. 2009a. Exploring the transition from wall slip to bulk shearing banding in well-entangled DNA solutions. *Soft Matter* 5:780–89
- Boukany PE, Wang SQ. 2009b. Shear banding or not in entangled DNA solutions depending on the level of entanglement. *J. Rheol.* 53:73–83
- Boukany PE, Wang SQ. 2010. Shear banding or not in entangled DNA solutions. *Macromolecules* 43:6950–52
- Britton MM, Callaghan PT. 1997. Two-phase shear band structures at uniform stress. *Phys. Rev. Lett.* 78:4930–33
- Buscall R. 2010. Letter to the editor: wall slip in dispersion rheometry. *J. Rheol.* 54:1177–83
- Callaghan PT. 2008. Rheo NMR and shear banding. *Rheol. Acta* 47:243–55
- Casanellas L, Dimitriou C, Ober TJ, McKinley G. 2015. Spatiotemporal dynamics of multiple shear-banding events for viscoelastic micellar fluids in cone-plate shearing flows. *J. Non-Newton. Fluid Mech.* 222:234–47
- Cates ME. 1990. Nonlinear viscoelasticity of wormlike micelles (and other reversibly breakable polymers). *J. Phys. Chem.* 94:371–75
- Cates ME, Fielding SM. 2006. Rheology of giant micelles. *Adv. Phys.* 55:799–879
- Chaudhuri P, Berthier L, Bocquet L. 2012. Inhomogeneous shear flows in soft jammed materials with tunable attractive forces. *Phys. Rev. E* 85:021503
- Chaudhuri P, Horbach J. 2013. Onset of flow in a confined colloidal glass under an imposed shear stress. *Phys. Rev. E* 88:040301
- Cheddadi I, Saramito P, Graner F. 2012. Steady Couette flows of elastoviscoplastic fluids are nonunique. *J. Rheol.* 56:213–39
- Chen LB, Chow MK, Ackerson BJ, Zukoski CF. 1994. Rheological and microstructural transitions in colloidal crystals. *Langmuir* 10:2817–29
- Cheng S, Wang SQ. 2012. Is shear banding a metastable property of well-entangled polymer solutions? *J. Rheol.* 56:1413–28
- Chikkadi V, Miedema D, Dang M, Nienhuis B, Schall P. 2014. Shear banding of colloidal glasses: observation of a dynamic first-order transition. *Phys. Rev. Lett.* 113:208301
- Christopoulou C, Petekidis G, Erwin B, Cloitre M, Vlassopoulos D. 2009. Ageing and yield behaviour in model soft colloidal glasses. *Philos. Trans. R. Soc. A* 367:5051–71
- Cloitre M, Borrega R, Leibler FML. 2003. Glassy dynamics and flow properties of soft colloidal pastes. *Phys. Rev. Lett.* 90:068303
- Coussot P, Nguyen QD, Huynh HT, Bonn D. 2002a. Viscosity bifurcation in thixotropic, yielding fluids. *J. Rheol.* 46:573–89
- Coussot P, Ovarlez G. 2010. Physical origin of shear-banding in jammed systems. *Eur. Phys. J. E* 33:183–88
- Coussot P, Raynaud JS, Bertrand F, Moucheron P, Guilbaud JP, et al. 2002b. Coexistence of liquid and solid phases in flowing soft-glassy materials. *Phys. Rev. Lett.* 88:218301
- Cromer M, Cook LP, McKinley GH. 2011. Interfacial instability of pressure-driven channel flow for a two-species model of entangled wormlike micellar solutions. *J. Non-Newton. Fluid Mech.* 166:566–77
- Cromer M, Fredrickson GH, Leal LG. 2014. A study of shear banding in polymer solutions. *Phys. Fluids* 26:063101
- de Gennes P. 1992. Soft matter (Nobel lecture). *Angew. Chem. Int. Ed. Engl.* 31:842–45
- Decruppe JP, Bécu L, Greffier O, Fazel N. 2010. Azimuthal instability of the interface in a shear banded flow by direct visual observation. *Phys. Rev. Lett.* 105:258301
- Dhont JKG. 1999. A constitutive relation describing the shear-banding transition. *Phys. Rev. E* 60:4534–44
- Diat O, Roux D, Nallet F. 1993. Effect of shear on a lyotropic lamellar phase. *J. Phys. II France* 3:1427–52
- Dimitriou CJ, Casanellas L, Ober TJ, McKinley GH. 2012. Rheo-PIV of a shear-banding wormlike micellar solution under large amplitude oscillatory shear. *Rheol. Acta* 51:395–411
- Divoux T, Barentin C, Manneville S. 2011. From transient fluidization processes to Herschel-Bulkley behavior in simple yield stress fluids. *Soft Matter* 7:8409–18

- Divoux T, Tamarii D, Barentin C, Manneville S. 2010. Transient shear banding in a simple yield stress fluid. *Phys. Rev. Lett.* 104:208301
- Divoux T, Tamarii D, Barentin C, Teitel S, Manneville S. 2012. Yielding dynamics of a Herschel-Bulkley fluid: a critical-like fluidization behaviour. *Soft Matter* 8:4151–64
- Doi M, Edwards S. 1988. *The Theory of Polymer Dynamics*. New York: Oxford Univ. Press
- Eberle AP, Porcar L. 2012. Flow-SANS and rheo-SANS applied to soft matter. *Curr. Opin. Colloid Interface Sci.* 17:33–43
- Eiser E, Molino F, Porte G, Diat O. 2000a. Nonhomogeneous textures and banded flows in a soft cubic phase under shear. *Phys. Rev. E* 61:6759–64
- Eiser E, Molino F, Porte G, Pithon X. 2000b. Flow in micellar cubic crystals. *Rheol. Acta* 39:201–8
- Fardin MA, Divoux T, Guedeau-Boudeville M, Buchet-Maulien I, Browaeys J, et al. 2012a. Shear-banding in surfactant wormlike micelles: elastic instabilities and wall slip. *Soft Matter* 8:2535–53
- Fardin MA, Lasne B, Cardoso O, Grégoire G, Argentina M, et al. 2009. Taylor-like vortices in shear-banding flow of giant micelles. *Phys. Rev. Lett.* 103:028302
- Fardin MA, Lerouge S. 2012. Instabilities in wormlike micelle systems: from shear banding to elastic turbulence. *Eur. Phys. J. E* 35:91
- Fardin MA, Lerouge S. 2014. Flows of living polymer fluids. *Soft Matter* 10:8789–99
- Fardin MA, Ober TJ, Gay C, Grégoire G, McKinley GH, Lerouge S. 2011. Criterion for purely elastic Taylor-Couette instability in the flows of shear-banding fluids. *Eur. Phys. Lett.* 96:44004
- Fardin MA, Ober TJ, Gay C, Grégoire G, McKinley GH, Lerouge S. 2012b. Potential ways of thinking about the shear-banding phenomenon. *Soft Matter* 8:910–22
- Fardin MA, Ober TJ, Grenard V, Divoux T, Manneville S, et al. 2012c. Interplay between elastic instabilities and shear-banding: three categories of Taylor-Couette flows and beyond. *Soft Matter* 8:10072–89
- Feindel KW, Callaghan PT. 2010. Anomalous shear banding: multidimensional dynamics under fluctuating slip conditions. *Rheol. Acta* 49:1003–13
- Fielding SM. 2007. Complex dynamics of shear banded flows. *Soft Matter* 3:1262–79
- Fielding SM. 2010. Viscoelastic Taylor-Couette instability of shear banded flow. *Phys. Rev. Lett.* 104:198303
- Fielding SM. 2011. Criterion for extensional necking instability in polymeric fluids. *Phys. Rev. Lett.* 107:258301
- Fielding SM. 2014. Shear banding in soft glassy materials. *Rep. Prog. Phys.* 77:102601
- Fielding SM, Olmsted PD. 2003. Flow phase diagrams for concentration-coupled shear banding. *Eur. Phys. J. E* 11:65–83
- Ganapathy R, Sood AK. 2006. Intermittency route to rheochaos in wormlike micelles with flow-concentration coupling. *Phys. Rev. Lett.* 96:108301
- Gibaud T, Barentin C, Manneville S. 2008. Influence of boundary conditions on yielding in a soft glassy material. *Phys. Rev. Lett.* 101:258302
- Gibaud T, Barentin C, Taberlet N, Manneville S. 2009. Shear-induced fragmentation of Laponite suspensions. *Soft Matter* 5:3026–37
- Gibaud T, Frelat D, Manneville S. 2010. Heterogeneous yielding dynamics in a colloidal gel. *Soft Matter* 6:3482–88
- Goddard JD. 2003. Material instability in complex fluids. *Annu. Rev. Fluid Mech.* 35:113–33
- Gopalakrishnan V, Zukoski C. 2007. Delayed flow in thermo-reversible colloidal gels. *J. Rheol.* 51:623–44
- Goyon J, Colin A, Ovarlez G, Ajdari A, Bocquet L. 2008. Flow cooperativity and breakdown of local constitutive laws for confined glassy flows. *Nature* 454:84–87
- Grenard V, Divoux T, Taberlet N, Manneville S. 2014. Timescales in creep and yielding of attractive gels. *Soft Matter* 10:1555–71
- Gurnon AK, Lopez-Barron C, Wasbrough MJ, Porcar L, Wagner NJ. 2014. Spatially resolved concentration and segmental flow alignment in a shear-banding solution of polymer-like micelles. *ACS Macro Lett.* 3:276–80
- Hamley I. 2001. Structure and flow behaviour of block copolymers. *J. Phys. Condens. Matter* 13:R643–71
- Hayes KA, Buckley MR, Cohen I, Archer LA. 2008. High resolution shear profile measurements in entangled polymers. *Phys. Rev. Lett.* 101:218301
- Hayes KA, Buckley MR, Qi H, Cohen I, Archer LA. 2010. Constitutive curve and velocity profile in entangled polymers during start-up of steady shear flow. *Macromolecules* 43:4412–17

- Helgeson ME, Reichert MD, Hu YT, Wagner NJ. 2009. Relating shear banding, structure, and phase behavior in wormlike micellar solutions. *Soft Matter* 5:3858–69
- Holmes WM, Callaghan PT, Vlassopoulos D, Roovers J. 2004. Shear banding phenomena in ultrasoft colloidal glasses. *J. Rheol.* 48:1085–102
- Hu YT. 2010. Steady-state shear banding in entangled polymers? *J. Rheol.* 54:1307–23
- Hu YT, Lips A. 2005. Kinetics and mechanism of shear banding in an entangled micellar solution. *J. Rheol.* 49:1001–27
- Irani E, Chaudhuri P, Heussinger C. 2014. Impact of attractive interactions on the rheology of dense athermal particles. *Phys. Rev. Lett.* 112:188303
- Jaradat S, Harvey M, Waigh TA. 2012. Shear-banding in polyacrylamide solutions revealed via optical coherence tomography velocimetry. *Soft Matter* 8:11677–86
- Larson RG. 1999. *The Structure and Rheology of Complex Fluids*. New York: Oxford Univ. Press
- Lerouge S, Berret JF. 2010. Shear-induced transitions and instabilities in surfactant wormlike micelles. *Adv. Polym. Sci.* 230:1–71
- Lerouge S, Decruppe JP, Berret JF. 2000. Correlation between rheological and optical properties of micellar solution under shear banding flow. *Langmuir* 16:6464–74
- Lerouge S, Decruppe JP, Olmsted PD. 2004. Birefringence banding in a micellar solution or the complexity of heterogeneous flows. *Langmuir* 20:11355–65
- Lerouge S, Fardin MA, Argentina M, Gregoire G, Cardoso O. 2008. Interface dynamics in shear-banding flow of giant micelles. *Soft Matter* 4:1808–19
- Lettinga MP, Manneville S. 2009. Competition between shear banding and wall slip in wormlike micelles. *Phys. Rev. Lett.* 103:248302
- Li Y, Hu M, McKenna GB, Dimitriou CJ, McKinley GH, et al. 2013. Flow field visualization of entangled polybutadiene solutions under nonlinear viscoelastic flow conditions. *J. Rheol.* 57:1411–28
- Li Y, Hu M, McKenna GB, Dimitriou CJ, McKinley GH, et al. 2014. Response to: Sufficiently entangled polymers do show shear strain localization at high enough Weissenberg numbers. *J. Rheol.* 58:1071–82
- Ligoure C, Mora S. 2013. Fractures in complex fluids: the case of transient networks. *Rheol Acta* 52:91–114
- López-González MR, Holmes WM, Callaghan PT, Photinos PJ. 2004. Shear banding fluctuations and nematic order in wormlike micelles. *Phys. Rev. Lett.* 93:268302
- López-González MR, Holmes WM, Callaghan PT, Photinos PJ. 2006. Rheo-NMR phenomena of wormlike micelles. *Soft Matter* 2:855–69
- Magnin A, Piau J. 1990. Cone-and-plate rheometry of yield stress fluids: study of an aqueous gel. *J. Non-Newton. Fluid Mech.* 36:85–108
- Mair RW, Callaghan PT. 1997. Shear flow of wormlike micelles in pipe and cylindrical Couette geometries as studied by nuclear magnetic resonance microscopy. *J. Rheol.* 41:901–23
- Manneville S. 2008. Recent experimental probes of shear banding. *Rheol. Acta* 47:301–18
- Manneville S, Colin A, Waton G, Schosseler F. 2007. Wall slip, shear banding, and instability in the flow of a triblock copolymer micellar solution. *Phys. Rev. E* 75:061502
- Marrucci G. 1996. Dynamics of entanglements: a nonlinear model consistent with the Cox-Merz rule. *J. Non-Newton. Fluid Mech.* 62:279–89
- Martin J, Hu Y. 2012. Transient and steady-state shear banding in aging soft glassy materials. *Soft Matter* 8:6940–49
- Masselon C, Colin A, Olmsted PD. 2010. Influence of boundary conditions and confinement on nonlocal effects in flows of wormlike micellar systems. *Phys. Rev. E* 81:021502
- Masselon C, Salmon JB, Colin A. 2008. Nonlocal effects in flows of wormlike micellar solutions. *Phys. Rev. Lett.* 100:038301
- McLeish T. 2002. Tube theory of entangled polymer dynamics. *Adv. Phys.* 51:1379–527
- McLeish T, Ball R. 1986. A molecular approach to the spurt effect in polymer melt flow. *J. Polym. Sci. B* 24:1735–45
- Menezes E, Graessley W. 1982. Nonlinear rheological behavior of polymer systems for several shear-flow histories. *J. Polym. Sci. Polym. Phys. Ed.* 20:1817–33
- Milner S, McLeish T, Likhtman A. 2001. Microscopic theory of convective constraint release. *J. Rheol.* 45:539–

- Møller PCF, Mewis J, Bonn D. 2006. Yield stress and thixotropy: on the difficulty of measuring yield stresses in practice. *Soft Matter* 2:274–83
- Møller PCF, Rodts S, Michels MAJ, Bonn D. 2008. Shear banding and yield stress in soft glassy materials. *Phys. Rev. E* 77:041507
- Moorcroft R, Cates M, Fielding S. 2011. Age-dependent transient shear banding in soft glasses. *Phys. Rev. Lett.* 106:055502
- Moorcroft R, Fielding S. 2013. Criteria for shear banding in time-dependent flows of complex fluids. *Phys. Rev. Lett.* 110:086001
- Morozov AN, van Saarloos W. 2007. An introductory essay on subcritical instabilities and the transition to turbulence in visco-elastic parallel shear flows. *Phys. Rep.* 447:112–43
- Muller SJ. 2008. Elastically-influenced instabilities in Taylor-Couette and other flows with curved streamlines: a review. *Korea-Aust. Rheol. J.* 20:117–25
- Nghe P, Fielding SM, Tabeling P, Ajdari A. 2010. Interfacially driven instability in the microchannel flow of a shear-banding fluid. *Phys. Rev. Lett.* 104:248303
- Nicolas A, Morozov A. 2012. Nonaxisymmetric instability of shear-banded Taylor-Couette flow. *Phys. Rev. Lett.* 108:088302
- Noirez L, Mendil-Jakani H, Baroni P. 2009. New light on old wisdoms on molten polymers: conformation, slippage and shear banding in sheared entangled and unentangled melts. *Macromol. Rapid Commun.* 30:1709–14
- Ober TJ, Soulages J, McKinley GH. 2011. Spatially resolved quantitative rheo-optics of complex fluids in a microfluidic device. *J. Rheol.* 55:1127–59
- Olmsted PD. 2008. Perspectives on shear banding in complex fluids. *Rheol. Acta* 47:283–300
- Ovarlez G, Rodts S, Chateau X, Coussot P. 2009. Phenomenology and physical origin of shear localization and shear banding in complex fluids. *Rheol. Acta* 48:831–44
- Paredes J, Shahidzadeh-Bonn N, Bonn D. 2011. Shear banding in thixotropic and normal emulsions. *J. Phys. Condens. Matter* 23:284116
- Pattamaprom C, Larson RG. 2001. Constraint release effects in monodisperse and bidisperse polystyrenes in fast transient shearing flows. *Macromolecules* 34:5229–37
- Perge C, Fardin MA, Manneville S. 2014. Surfactant micelles: model systems for flow instabilities of complex fluids. *Eur. Phys. J. E* 37:23–34
- Picard G, Ajdari A, Bocquet L, Lequeux F. 2002. A simple model for heterogeneous flows of yield stress fluids. *Phys. Rev. E* 66:051501
- Pignon F, Magnin A, Piau JM. 1996. Thixotropic colloidal suspensions and flow curves with minimum: identification of flow regimes and rheometric consequences. *J. Rheol.* 40:573–87
- Radulescu O, Olmsted PD. 1999. Matched asymptotic solutions for the steady banded flow of the diffusive Johnson-Segalman model in various geometries. *J. Non-Newton. Fluid Mech.* 91:143–64
- Radulescu O, Olmsted PD, Decruppe JP, Lerouge S, Berret JF, Porte G. 2003. Time scales in shear banding of wormlike micelles. *Europhys. Lett.* 62:230–36
- Radulescu O, Olmsted PD, Lu CYD. 1999. Shear banding in reaction-diffusion models. *Rheol. Acta* 38:606–13
- Ragouilliaux A, Herzhaft B, Bertrand F, Coussot P. 2006. Flow instability and shear localization in a drilling mud. *Rheol. Acta* 46:261–71
- Ragouilliaux A, Ovarlez G, Shahidzadeh-Bonn N, Herzhaft B, Palermo T, Coussot P. 2007. Transition from a simple yield-stress fluid to a thixotropic material. *Phys. Rev. E* 76:051408
- Ravindranath S, Wang SQ, Ofecnovic M, Quirk RP. 2008. Banding in simple steady shear of entangled polymer solutions. *Macromolecules* 41:2663–70
- Rehage H, Hoffmann H. 1991. Viscoelastic surfactant solutions: model systems for rheological research. *Mol. Phys.* 74:933–73
- Rogers SA, Callaghan P, Petekidis G, Vlassopoulos D. 2010. Time-dependent rheology of colloidal star glasses. *J. Rheol.* 54:133–58
- Rogers SA, Vlassopoulos D, Callaghan PT. 2008. Aging, yielding, and shear banding in soft colloidal glasses. *Phys. Rev. Lett.* 100:128304
- Roux D, Nallet F, Diat O. 1993. Rheology of lyotropic lamellar phases. *Europhys. Lett.* 24:53–58

- Salmon JB, Colin A, Manneville S, Molino F. 2003a. Velocity profiles in shear-banding wormlike micelles. *Phys. Rev. Lett.* 90:228303
- Salmon JB, Manneville S, Colin A. 2003b. Shear banding in a lyotropic lamellar phase. I. Time-averaged velocity profiles. *Phys. Rev. E* 68:051503
- Schall P, van Hecke M. 2010. Shear bands in matter with granularity. *Annu. Rev. Fluid Mech.* 42:67–88
- Seth J, Locatelli-Champagne C, Monti F, Bonnecaze R, Cloitre M. 2012. How do soft particle glasses yield and flow near solid surfaces? *Soft Matter* 8:140–48
- Shereda L, Larson R, Solomon M. 2010. Shear banding in crystallizing colloidal suspensions. *Korea-Aust. Rheol. J.* 22:309–16
- Skrzeszewska P, Sprakel J, de Wolf F, Fokink R, Stuart MC, van der Gucht J. 2010. Fracture and self-healing in a well-defined self-assembled polymer network. *Macromolecules* 43:3542–48
- Spenley A, Yuan XF, Cates ME. 1996. Nonmonotonic constitutive laws and the formation of shear-banded flows. *J. Phys. II France* 6:551–71
- Sprakel J, Lindström S, Kodger T, Weitz D. 2011. Stress enhancement in the delayed yielding of colloidal gels. *Phys. Rev. Lett.* 106:248303
- Tsamados M. 2010. Plasticity and dynamical heterogeneity in driven glassy materials. *Eur. Phys. J. E* 32:165–81
- van der Noort A, Briels W. 2008. Brownian dynamics simulations of concentration coupled shear banding. *J. Non-Newton. Fluid Mech.* 152:148–55
- Varnik F, Bocquet L, Barrat JL, Berthier L. 2003. Shear localization in a model glass. *Phys. Rev. Lett.* 90:095702
- Vinogradov G. 1973. Critical regimes of deformation of liquid polymeric systems. *Rheol. Acta* 12:357–73
- Vlassopoulos D, Fytas G. 2010. From polymers to colloids: engineering the dynamic properties of hairy particles. *Adv. Polym. Sci.* 236:1–54
- Wang SQ. 2009. Comment on “Nonmonotonic models are not necessary to obtain shear banding phenomena in entangled polymer solutions.” *Phys. Rev. Lett.* 103:219801
- Wang SQ, Liu G, Cheng S, Boukany PE, Wang Y, Li X. 2014. Letter to the editor: Sufficiently entangled polymers do show shear strain localization at high enough Weissenberg numbers. *J. Rheol.* 58:1059–69
- Wang SQ, Ravindranath S, Boukany PE. 2011. Homogeneous shear, wall slip, and shear banding of entangled polymeric liquids in simple-shear rheometry: a roadmap of nonlinear rheology. *Macromolecules* 44:183–90
- Wright TW. 2002. *The Physics and Mathematics of Adiabatic Shear Bands*. Cambridge, UK: Cambridge Univ. Press
- Xu A, Gonnella G, Lamura A. 2006. Morphologies and flow patterns in quenching of lamellar systems with shear. *Phys. Rev. E* 74:011505
- Yerushalmi J, Katz S, Shinnar R. 1970. Stability of steady shear flows of some viscoelastic fluids. *Chem. Eng. Sci.* 25:1891–902
- Zhou L, McKinley GH, Cook LP. 2014. Wormlike micellar solutions: III. VCM model predictions in steady and transient shearing flows. *J. Non-Newton. Fluid Mech.* 211:70–83
- Zhu X, Yang W, Wang SQ. 2013. Exploring shear yielding and strain localization at the die entry during extrusion of entangled melts. *J. Rheol.* 57:349–64
- Zou W, Larson RG. 2014. A mesoscopic simulation method for predicting the rheology of semi-dilute wormlike micellar solutions. *J. Rheol.* 58:681–721